LIQUEFACTION OF DEEP SATURATED SANDS UNDER HIGH EFFECTIVE CONFINING STRESS

R Scott Steedman
Whitby Bird & Partners
60 Newman Street,
London, UK

Michael Sharp
US Army
Engineer Research & Development Center
Vicksburg, MS

ABSTRACT

This paper describes the findings of an ongoing experimental study supported by the U.S. Army Centrifuge Research Center and Engineer Earthquake Engineering Research Program (EQEN) into the behavior of saturated sands under high initial effective confining stresses subjected to strong ground shaking. The research was conducted using the Army Centrifuge at the U.S. Army Engineering Research and Development Center (ERDC), located in Vicksburg MS, formerly known as the Waterways Experiment Station (WES). The centrifuge studies have shown that the generation of excess pore pressure is limited to a level below 100 percent for vertical effective confining stresses exceeding around 3 atmospheres (atm, or 300 KPa). This limit reduces at higher confining stresses. One explanation may be linked to the effects of drainage up through the soil column. If verified, the potential benefits from this finding for the design of remediation works for large earth dams or other deep sites could be substantial. The paper describes the equipment used for the experiments, the research program, and presents the initial results, contrasting the development of excess pore pressure at low confining stress with that at high confining stress.

INTRODUCTION

The current state-of-practice for the evaluation of liquefaction potential and for remediation design and analysis depends on empirical correlations of in-situ measurements of strength versus field experience of liquefaction at shallow depth and laboratory data of the behavior of confined elements under cyclic loading. (Liquefaction is defined here to mean the development of pore pressure equal to 100% of the initial vertical effective stress.) This approach is known as the "simplified procedure". Opinions vary as to the maximum depth in the field at which liquefaction has been observed, but there is no established field evidence from historic earthquakes of liquefaction at depths greater than a few tens of meters. The NCEER Workshop in 1996 on the Evaluation of Liquefaction Resistance of Soils noted that the simplified procedure was developed from evaluations of field observations and field and laboratory test data, Youd and Idriss (1997). The report notes, "These data were collected mostly from sites … at shallow depths (less than 15m). The original procedure was verified for and is applicable only to these site conditions".

Hence, in design practice the assessment of liquefaction under high initial effective confining stress, such as might relate to the foundations of large earth dams, is based on the extrapolation of observed behavior and correlations at shallow depths. In practice, the behavior of saturated soil under these conditions is not well understood. Based on the results of laboratory tests, researchers have postulated that there is a reduction in the liquefaction resistance of such soil compared to shallow depths. Laboratory element tests clearly show that with sufficient numbers of cycles of sufficient strain amplitude, excess pore pressures in an undrained specimen, even under high initial effective confining stress will reach a level associated with initial liquefaction.

Centrifuge model experiments provide an opportunity to investigate the behavior of fine sands under strong ground shaking in the context of a particular field geometry or soil profile. In the absence of field data, centrifuge model experiments are now used routinely to investigate soil-structure interaction problems and provide verification for design techniques. The centrifuge facility at ERDC has been operational for some years now, and is equipped with a large mechanical shaker designed for operation at g levels of up to 150g. The ERDC centrifuge and Mk I earthquake shaker were described by Steedman et al. (2000).

The object of the experiments carried out under this research

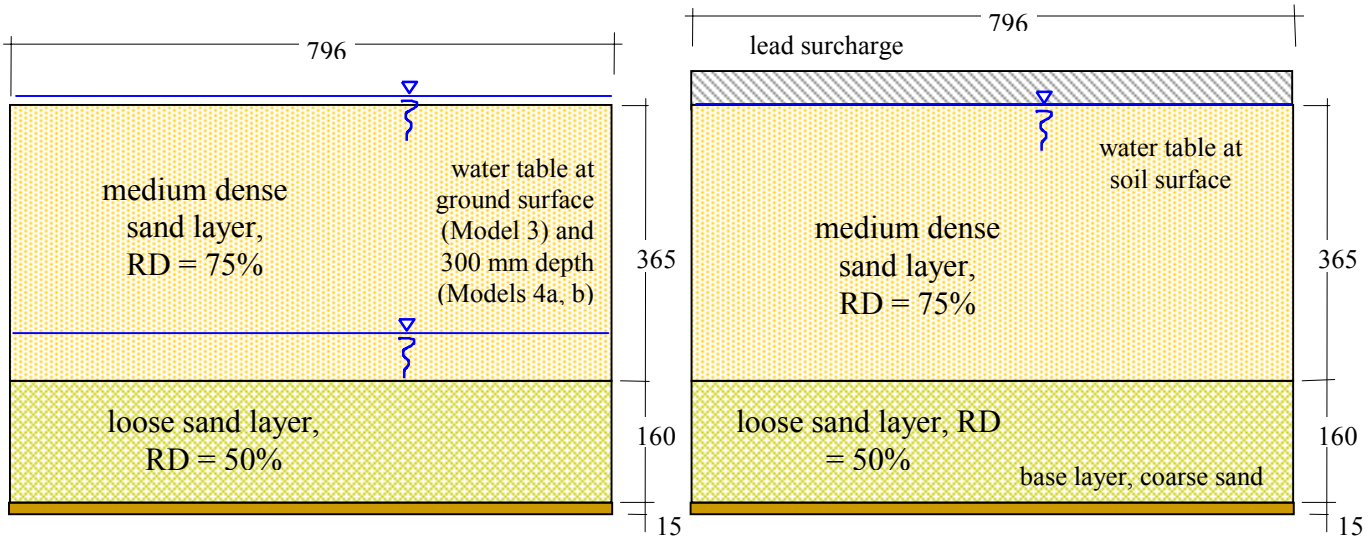

Typical cross section: Models 3 and 4 a, b

Typical cross section: Models 4 c, d, f and 5 a-d

program was to explore the development of excess pore pressure in loose saturated sands under initial confining stresses ranging from 100 KPa (1 tsf) up to 1000 KPa (10 tsf). The specimens were designed to model either the full depth of soil deposit in the field, or a substantial depth above and below a 'target' loose layer. Figure 1 shows typical cross-sections through the different model specimens.

Figure 1. Typical cross sections through the model specimens.

The liquefaction of a level sand bed has previously been the subject of other research. Experiments were conducted at many centrifuge centers under the VELACS project, Arulanandan and Scott (1994). The studies at ERDC to date have focused on level ground initial stress conditions in a two-layer (dense over loose) deposit of clean, fine Nevada sand. Recent experiments have adopted a uniform density throughout the depth. Examination of more complex stratigraphy and sloping ground stress conditions is planned for future studies.

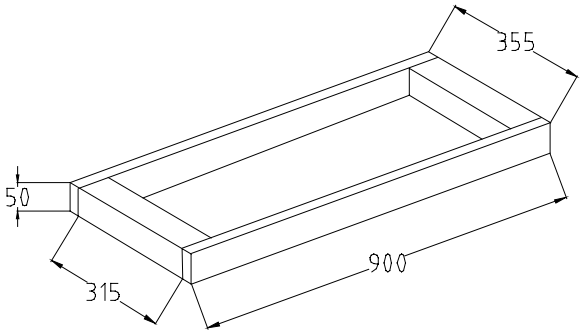

Figure 2. Typical Equivalent Shear Beam specimen container

Thin metal sheets, termed shear sheets, are positioned on the interior end walls of the chamber and fixed securely to its base. The shear sheets accommodate the complementary shear force generated by the horizontal shaking within the specimen and transmit that force to the base of the container, Figure 3. This improves the uniformity of the stress field at each elevation along the model, reducing the tendency for the chamber to 'rock'.

Model containment

The specimens were built within a hollow rectangular model container, termed an equivalent shear beam (ESB) container, comprising a series of eleven aluminium alloy rings stacked one above the other, and separated by an elastic medium, Figure 2. Several of these chambers have been constructed, and extensive dynamic analysis and testing has been carried out to determine their dynamic response characteristics, Butler (1999). The model container has internal dimensions of 627mm deep by 315mm wide by 796mm long. Each of the eleven aluminium alloy rings is 50mm high. The rings are not stiff enough along their long dimension to support the outward pressure from the soil inside under high g, but they are supported by the massive reaction walls of the shaker unit itself. A rubber sheet separates the rings from the steel walls on either side. This concept has the added advantage of raising the center of gravity of the reaction mass in line with the center of gravity of the specimen, thus minimizing eccentric forces that may lead to rocking.

The ESB concept is to create an equivalent shear beam with an average stiffness comparable to the stiffness of the soil specimen. Expressed rigorously, the concept is more accurately defined as achieving a dynamic response that does not significantly influence the behavior of the soil specimen inside. The ERDC ESB used in these experiments was assembled using a urethane adhesive sealant (commonly used as a windshield sealant for cars) between the aluminum alloy rings. This material has good elastic properties (exhibiting only minimal hysteresis under cyclic loading) and bonded well to the metal and to itself. The ESB has a relatively low shear stiffness of 441 KN/m^2 (shear stiffness of the full stacked ring assembly) and mass of 229 kg, with a first mode at 16Hz, and second, third, and fourth modes at 46, 87, and 116Hz respectively (Butler 1999). A typical saturated specimen at 50g in the ERDC ESB will have a theoretical natural frequency of around 84Hz, based on an average small strain shear modulus of 96 MN/m^2. Further discussion of the dynamic response of the ERDC model container, and the benefits and challenges of the ESB concept, was reported by Steedman et al. (2000).

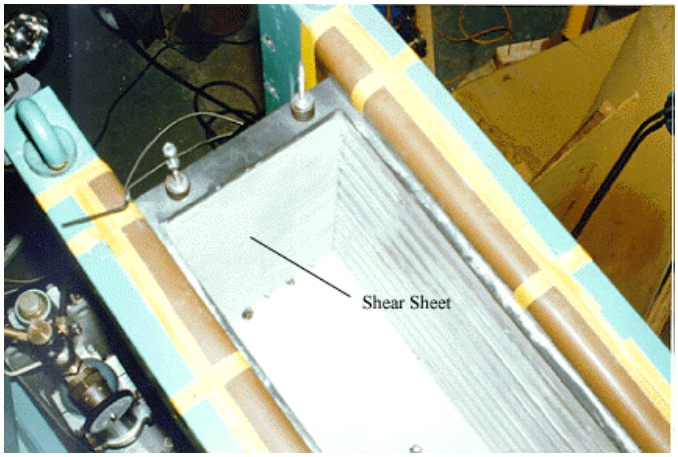

Figure 3. Shear sheets form the boundaries on the end walls of the ESB

RESEARCH PROGRAM

Table 1 summarises the different series of experiments conducted from 1998 – 2000. Each series corresponds to a different target range of vertical effective overburden stress in the loose layer. Most specimens comprised a loose layer of 160mm deep overlain by a denser layer of either 140mm or 365mm depth. A few verification specimens were of uniform density throughout their depth. Similarly, most models were shaken at 50g. To achieve the highest effective overburden stress, some models used a lead surcharge; others were tested at higher gravity level, up to 125g. Some models were overconsolidated by a factor of 2.5 prior to shaking (achieved by running the centrifuge up to 125g). A large series of experiments have been conducted with a range of overburden depths to provide repeatability and redundancy in the instrumentation and data records. Base information for each individual specimen is summarized in Table 2.

Model series	Models in series	Effective overburden stress in loose layer	Equivalent field depth (approx)	Depth of specimen	Notes (all specimens constructed from Nevada Sand and were tested at 50g unless indicated)
2	a, b, c, d, e, f	1 tsf	15 m	300 mm	
3	a, b, c, d, e	2 tsf	26 m	525 mm	
4	a, b, c, d	3 – 5 tsf	26 – 40 m	525 mm	With lowered w.t. or surcharge
	e, f, g, h, i, j	3.9 – 9.7 tsf	30 – 60 m	525 mm	With light surcharge and change in g level
	k	1.9 – 4.8 tsf	25 – 39 m	525 mm	With change in g level
5	a, b, c, d, e	7 – 10 tsf	54 – 63 m	525 mm	With lead surcharge

Table 1. Summary of model tests

Model Code	Overall depth (mm)	Relative Density (RD)	σ_v' at mid-depth in loose layer (tsf)	OCR	Number of earth-quakes	Comments *All specimens constructed from Nevada Sand and tested at 50g unless specified*. Depth of loose layer 160mm unless uniform density.*
2a	300	44% loose, 83% dense	1	1	3	Saturated to ground surface.
2b	300	50% loose, 75% dense	1	1	2	Saturated to ground surface.
2c	300	49% loose, 74% dense	1	1	5	Saturated to ground surface.
2d	300	50% loose, 75% dense	1	1	4	Saturated to ground surface.
2e	300	49% loose, 73% dense	1	2.5	4	Saturated to ground surface.
2f	300	50% loose, 75% dense	1	2.5	4	Saturated to ground surface.
3a	525	34% loose, 73% dense	2	1	2	Saturated to ground surface.
3b	525	49% loose, 77% dense	2	1	3	Saturated to ground surface.
3c	525	49% loose, 79% dense	2	1	3	Saturated to ground surface.
3d	525	54% loose, 80% dense	2	2.5	4	Saturated to ground surface.
4a	525	49% loose, 80% dense	3	1	4	Saturated to top of loose layer only.
4b	525	56% loose, 74% dense	3	2.5	4	Saturated to top of loose layer only.
4c	525	50% loose, 75% dense	4.7	1	4	Saturated to ground surface. Lead surcharge.
4d	525	50% loose, 68% dense	4.7	2.5	4	Saturated to ground surface. Lead surcharge.
4e	525	47% uniform	3.9 – 7.8	1	2,1,1*	Saturated to ground surface. Light surcharge in three strips. *Shaking at 50, 80, 100g.
4f	525	75% upper, 45% lower	3.9 – 9.7	1	1,1,2,1*	Saturated to ground surface. Light surcharge in three strips. *Shaking at 50, 80, 100, 125g.
4g	525	50% uniform	3.9 – 9.7	1	1,1,1,2*	Saturated to ground surface. Light surcharge in three strips. *Shaking at 50, 80, 100, 125g.
4h	525	50% uniform	3.9 – 9.7	1	1,1,1,1*	Saturated to ground surface. Light surcharge in three strips. *Shaking at 50, 80, 100, 125g.
4i	525	50% uniform	3.9 – 9.7	1	1,1,1,1*	Saturated to ground surface. Light surcharge in three strips. *Shaking at 50, 80, 100, 125g.
4j	525	50% uniform	3.9 – 9.7	1	1,1,1,2*	Saturated to ground surface. Light surcharge in three strips. *Shaking at 50, 80, 100, 125g.
4k	525	50% uniform	1.9 – 4.8	1	1,1,1,2*	Saturated to ground surface. No surcharge. *Shaking at 50, 80, 100, 125g.
5a	525	51% loose, 72% dense	7.4	1	4	Saturated to ground surface. Lead surcharge.
5b	525	49% loose, 76% dense	7.4	2.5	4	Saturated to ground surface. Lead surcharge.
5c	525	52% loose, 75% dense	9.2	1	3	Saturated to ground surface. Lead surcharge.
5d	525	57% loose, 80% dense	9.2	1	1	Saturated to ground surface. Lead surcharge.
5e	525	c. 50% uniform	8.4	1	7	Saturated to ground surface. Lead surcharge.

Table 2. Detailed summary of experiments

The Nevada sand used in the models was characterized by standard laboratory tests to determine parameters such as dry density and gradation, Table 3. The pore fluid comprised a mixture of glycerine and water, 80% by weight for experiments conducted at 50g. Table 4 summarizes the properties of the glycerine-water solution used as the pore fluid.

Maximum void ratio	0.757 (density 93.8 pcf)
Minimum void ratio	0.516 (density 108.7 pcf)
D_{50}	0.18 mm (approx)
D_{10}	0.11 mm (approx)
Specific gravity	2.64

Table 3. Nevada Sand (parameters as measured)

Density	1200 kg/m^3
Viscosity	50 cs
Specific Gravity	1.26
Composition	80% glycerine-water mix (by weight)

Table 4. Parameters for pore fluid (as measured)

The models were poured dry from a hopper and saturated under vacuum, or slowly under gravity. Instrumentation was placed in the model as it was being constructed.

Instrumentation was positioned through the depth of the models, and comprised pore pressure transducers and accelerometers.

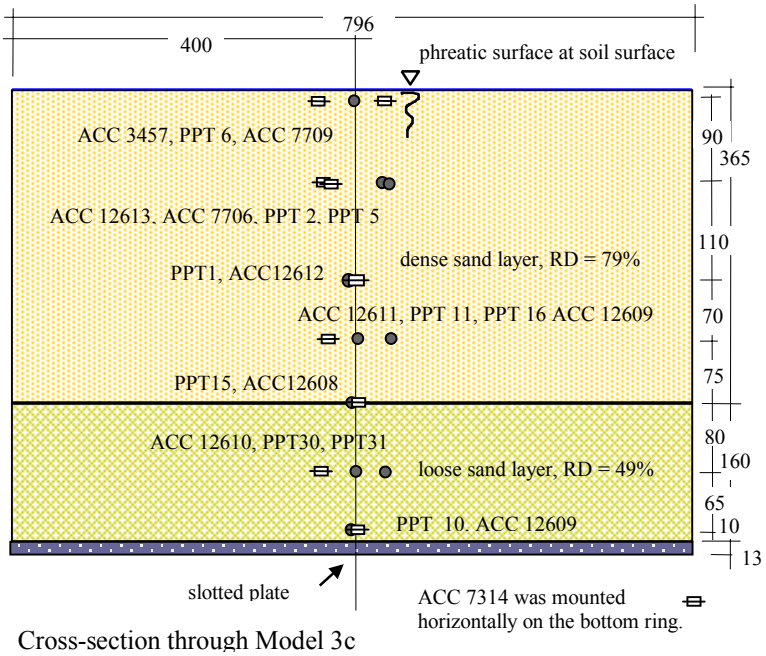

Cross-section through Model 3c

The location of the instrumentation for Model 3c is shown in Figure 4.

Figure 4. Instrumentation for Model 3c

DEVELOPMENT OF EXCESS PORE PRESSURES AND LIQUEFACTION AT SHALLOW DEPTHS

The target initial effective vertical stress in Model 3c was 200 KPa (2 tsf) at mid-depth in the loose layer (Table 1). The specimen was normally consolidated by accelerating the centrifuge and subject to shaking motion at 50g. Figure 5 shows how the accelerations at different depths are affected by the excess pore pressures during the shaking. It is clear that within a few cycles of shaking, the loose sand layer has fully liquefied and the upper transducers are effectively isolated from the base input shaking.

Comparison between the acceleration time histories in Figure 5 and the excess pore pressures in Figure 6 for the loose and dense layers shows the correlation between transmitted motion and level of excess pore pressure. The upper section (near surface) of the dense layer liquefies within 0.2 seconds (0.2 x 50 = 10 seconds field equivalent). The percentage of excess pore pressure is calculated by dividing the measured fluid pressure by the calculated initial overburden stress. The actual overburden stress may vary over time due to small movements of the transducer in the liquefied ground; this has a larger effect on the accuracy of measurement at shallower locations, such as PPT 2.

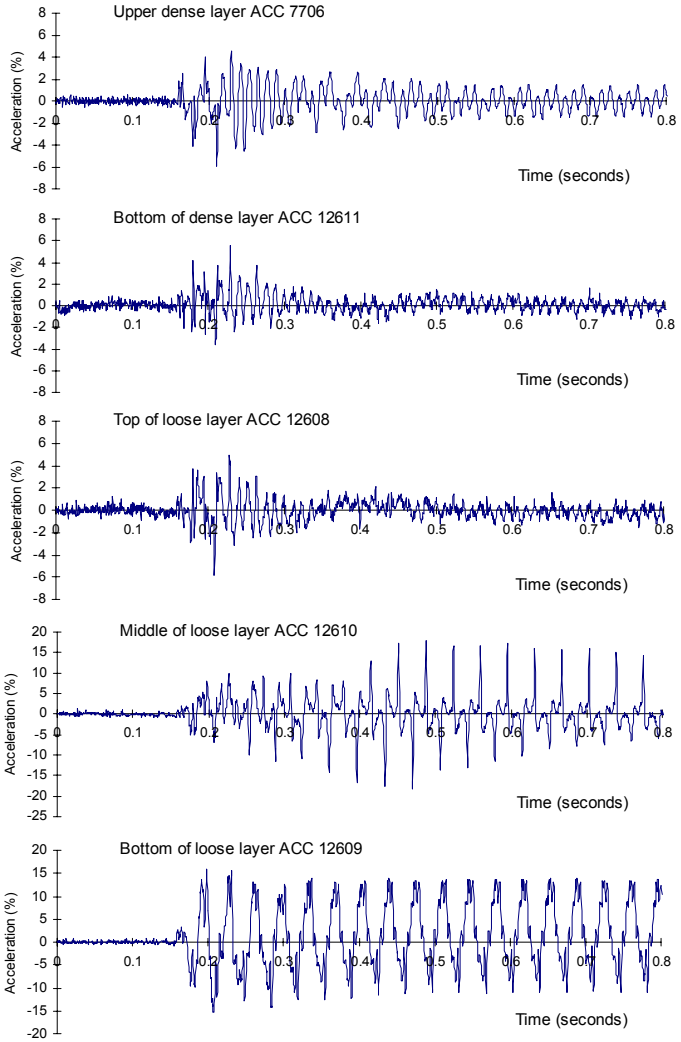

Figure 5. Time histories of acceleration: Model 3c

It is interesting to note that despite the difference in relative

density between the dense and loose layers, the soil column behaves more like a single unit than as two layers.

The almost instantaneous transmission of high excess pore pressures from the lower loose layers into the upper dense layers, readily causing the upper layer to liquefy also, is most likely due to the stiffness of the pore fluid (similar to water) and the high level of saturation. Coupled stress-flow effective stress analyses conducted at UBC confirm that transmission of excess pore pressure in such a layered profile is necessary to satisfactorily predict the response of the upper layers, Byrne (2001).

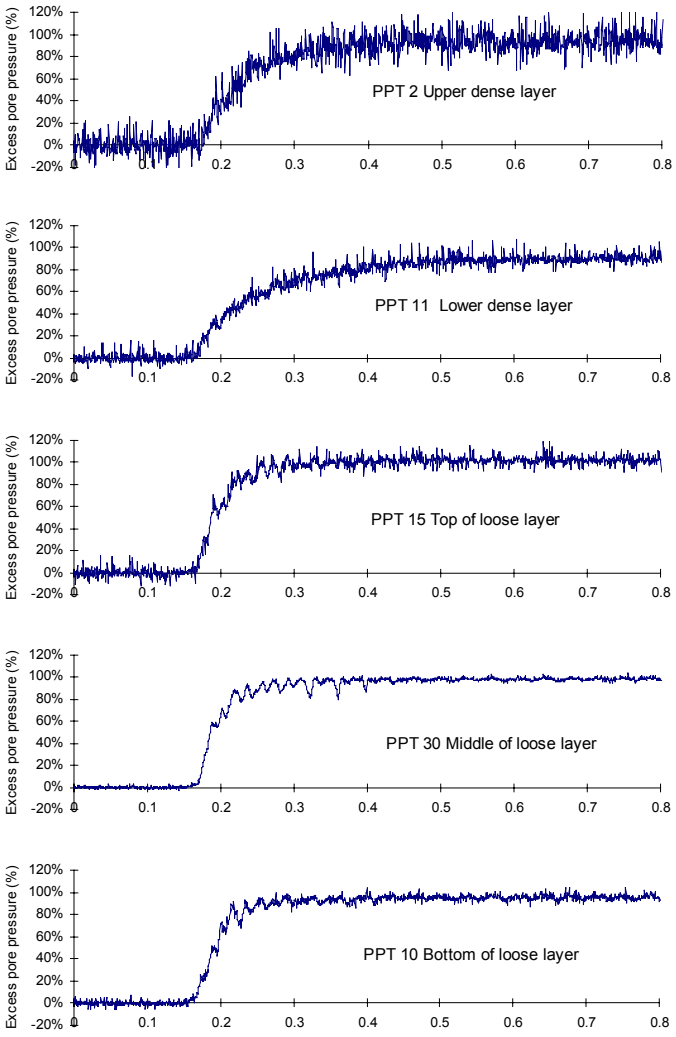

Figure 6. Time histories of excess pore pressure: Model 3c

COMPARISON OF LAYERED DENSE OVER LOOSE AND UNIFORM LOOSE SOIL PROFILES

The observation of high excess pore pressures in the dense layer, driven by the development of excess pore pressures beneath was further demonstrated by comparison between a layered specimen (such as Model 3c) and a uniform loose specimen (Model 4k). The general cross section through the specimens shows the location of the loose and dense layers, Figure 7. Comparison between the excess pore pressures at homologous locations shows a close similarity between the two specimens, despite differences in the amplitude and frequency of the input base shaking, Figure 8.

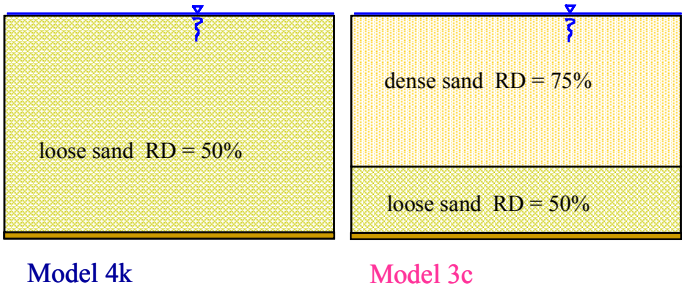

Figure 7. Cross sections through layered and uniform models

Figure 8. Comparison between excess pore pressure in

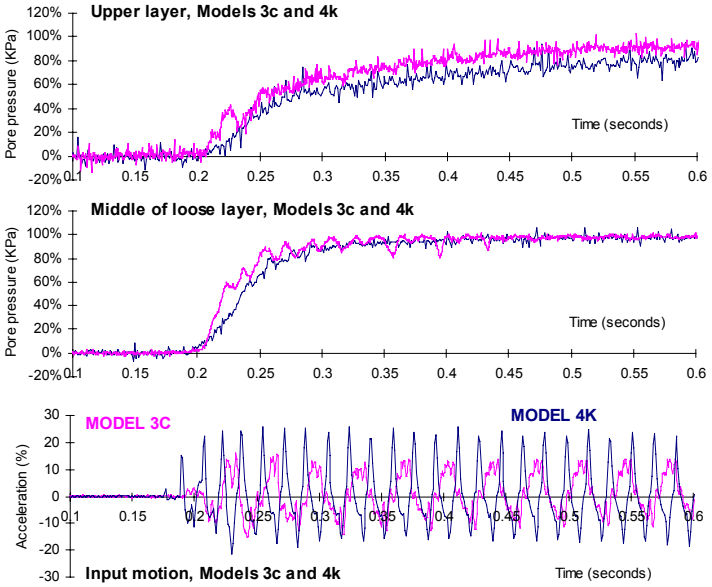

layered and uniform models

GENERATION OF EXCESS PORE PRESSURES AT HIGH CONFINING STRESS

At high initial effective confining stress excess pore pressures are also observed to rise strongly during the initial cycles of shaking. After some time, this steady rise is arrested, and then excess pore pressure is capped at a value less than the full 100% of the initial vertical effective stress seen in shallow soil columns. Figure 10 shows a set of data from Model 5e, a deep soil specimen with an initial effective vertical stress of around 1000 KPa (9.7 tsf) at mid-depth in the loose layer. Despite the large amplitude of shaking (a mean base input in excess of 30%g at a field equivalent depth greater than 60m) a marked transition in behavior occurs around 0.3 seconds (15 seconds field equivalent) into the event, and the rate of rise of excess pore pressure suddenly drops to near zero. This sharply bilinear character in the

pore pressure response was pronounced at all levels of initial effective confining stress.

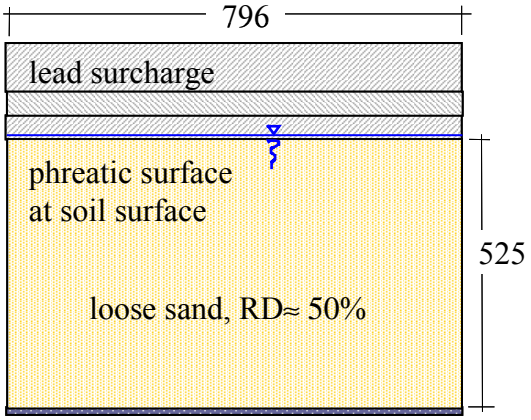

Figure 9. Cross-section through Model 5e

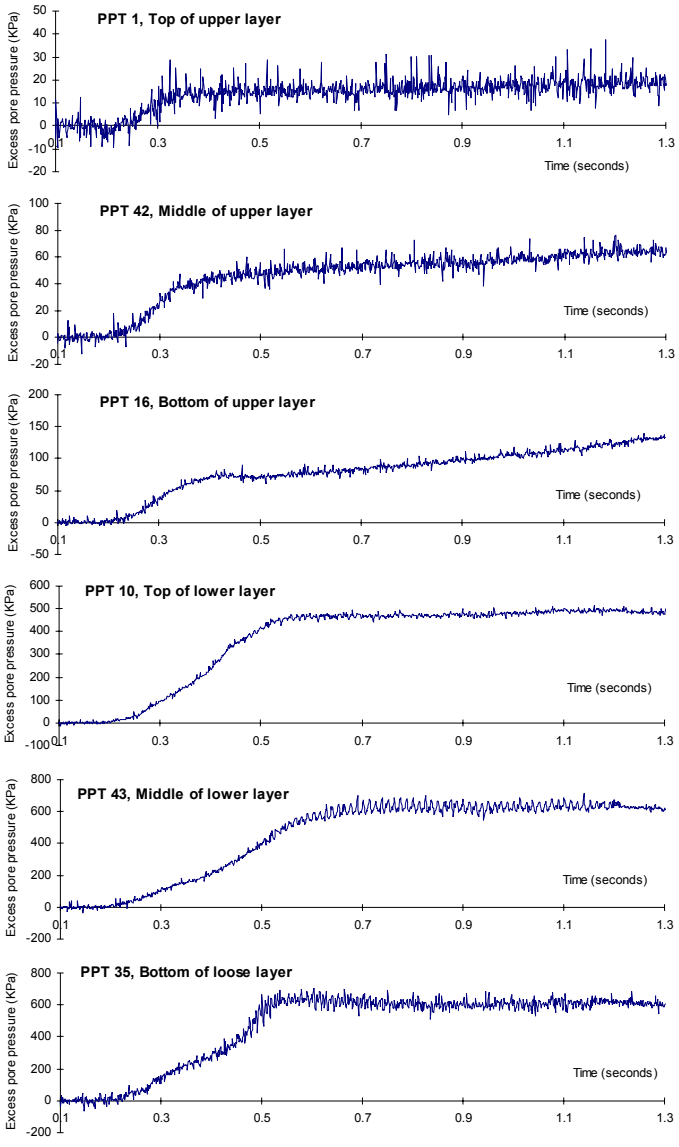

Figure 10. Time histories of excess pore pressure, Model 5e

This pattern of behavior was found in all specimens at initial vertical effective confining stresses of around 250 KPa or greater. Although not a rigorous comparison, as there are a number of variables (including amplitude) between the different experiments, Figure 11 shows the normalised results from a range of initial conditions. There is a general trend with increasing initial vertical effective stress, towards the limiting of excess pore pressure at a level lower than the expected 100%.

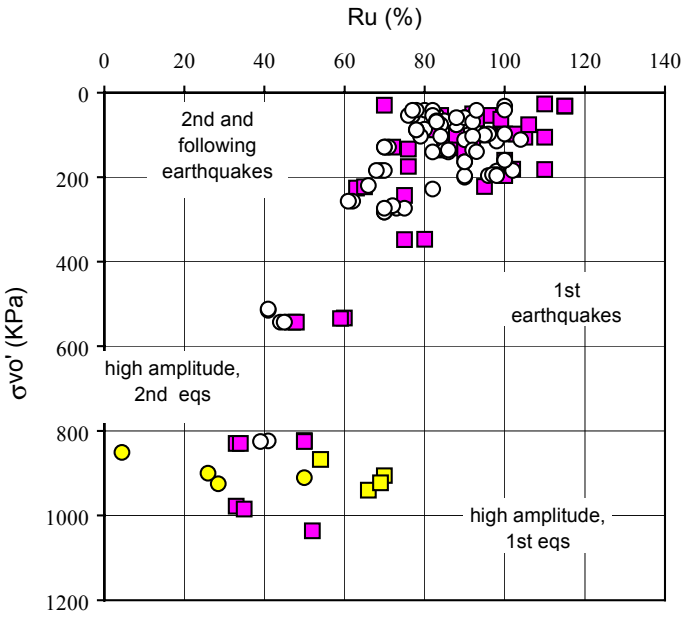

Figure 11. Limiting Ru (%) as a function of initial vertical effective stress (KPa)

A number of models, including 5e, were subject to high amplitude base shaking. They showed a higher limiting Ru than similar specimens subject to lower amplitude shaking. Second and following earthquakes showed a reduced level of limiting Ru, as compared to the first earthquake data, as would be expected.

DETERMINATION OF SHEAR STRESS-STRAIN PROPERTIES

The cyclic properties of soils depend on the state of stress in the soil prior to loading and on the stresses imposed by the loading. Since the testing reported in this paper refers only to level ground conditions, there is no initial static shear stress and hence no need to account for such. The only shear stress and subsequent shear strain is that imposed by the loading. The results reported in this paper, level ground liquefaction, are a special case of the cyclic mobility phenomenon that occurs when the static shear stress is less than the shear strength of the liquefied soil. Level ground liquefaction failures are caused by the upward flow of water that occurs when seismically induced excess pore pressures dissipate. Depending on the length of time

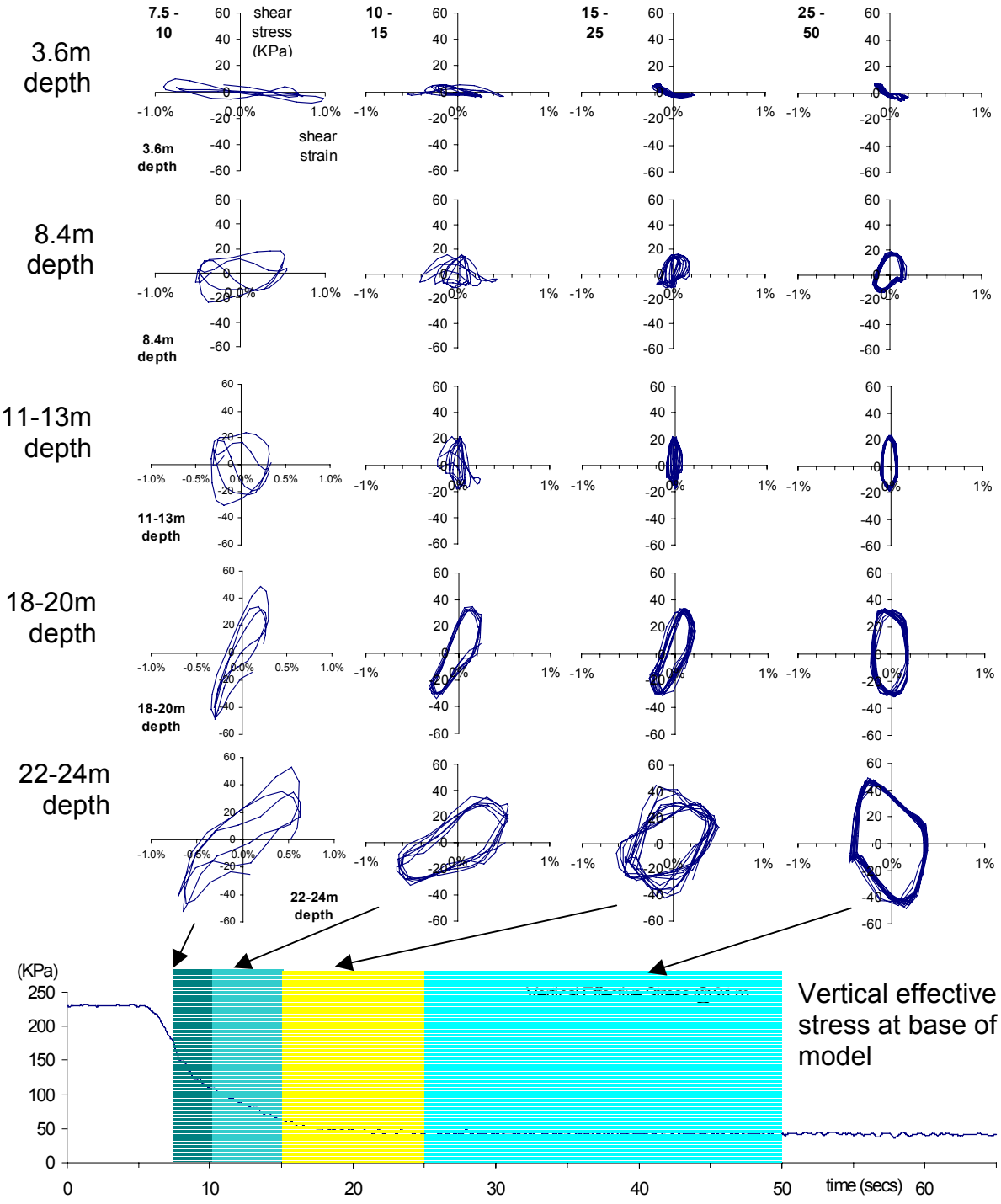

required to reach hydraulic equilibrium, level ground liquefaction failure may occur well after ground shaking has ceased.

Figure 12. Stress strain time histories, Model 4k

It was considered that a critical aspect in the assessment of these model experiments was to compute the stress strain time histories for comparison with laboratory element and field experience.

Zeghal et. al. (1995), proposed that accelerometer and pore pressure time histories could offer a direct and effective means of evaluating seismic soil properties, in particular, a second order accurate estimation of shear stress and shear strain. This technique has been termed System Identification (SI), and has been utilized for analysis of data reported in this paper. The SI technique was described in detail by Zeghal et al. (1995).

Analysis of the test results from all models reported in Table 2 is currently ongoing. This analysis includes traditional techniques, SI, and numerical modeling. Stress strain figures are shown here for Models 4k (Figure 7) and 5b (similar in cross section to 5e,

Figure 9), windowed during similar stages of shaking.

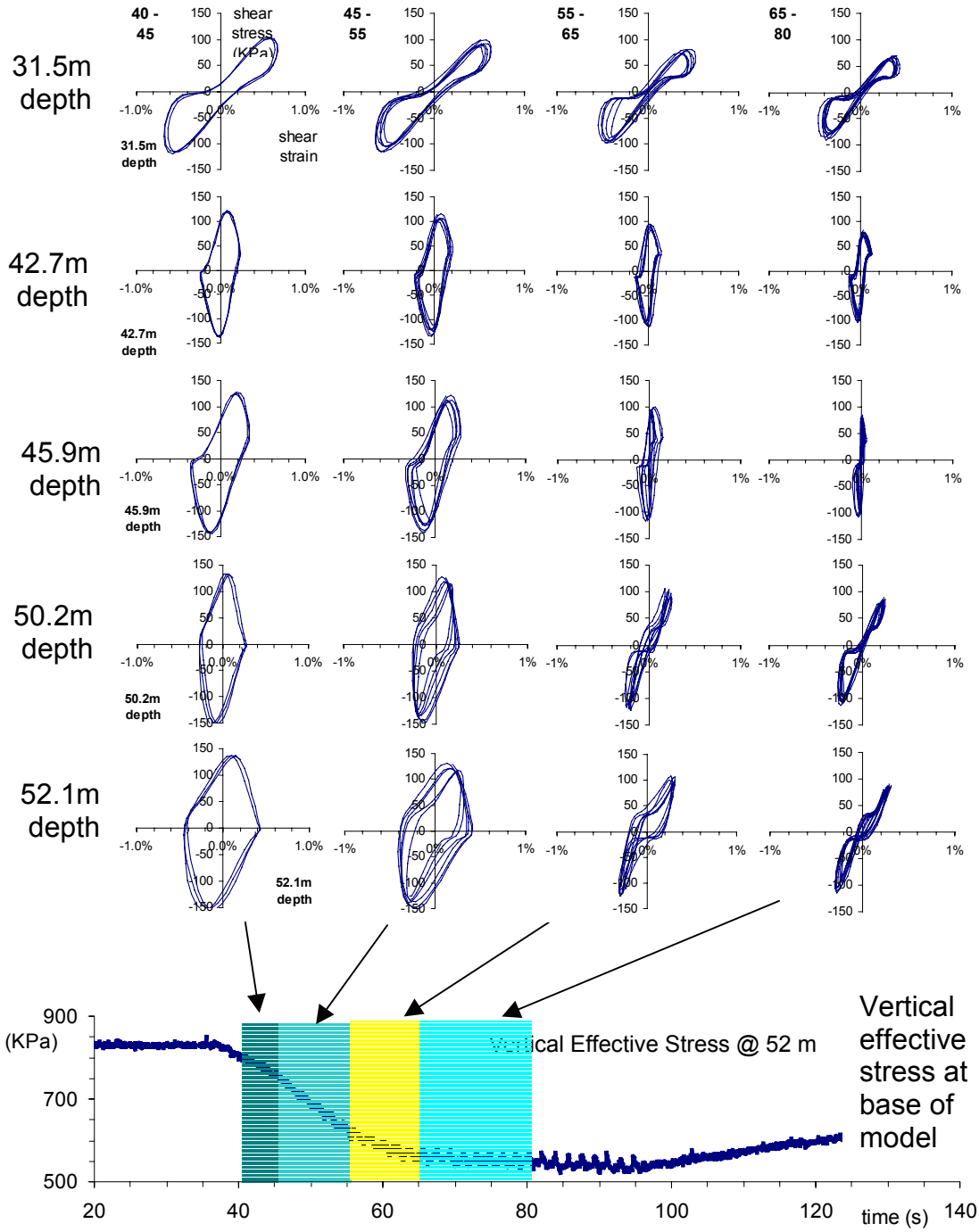

Figure 13. Stress strain time histories, Model 5b

The left column of plots are the traditional stress-strain loops computed for the early time data, as the excess pore pressures are developing strongly. This may be seen by comparison with the time history of vertical effective stress below the stress strain figures. For Model 4k this shows the largest amount of straining near the surface at nearly 1%, decreasing to a strain of 0.6% at a depth of 24 m. The remaining columns of figures show how the stress strain loops are altered by the development of excess pore pressure. In the case of Model 4k, the specimen reaches close to 100% excess pore pressure, and the upper layers become isolated from the straining at the base. In the case of Model 5b, the excess pore pressure is limited and the response of the soil column becomes nearly linear. The marked contrast in response between the two specimens confirm the observation that the stabilization of the excess pore pressure development in the deeper specimens is a genuine phenomenon associated with a stable cycling of applied load at a level significantly below 100% excess pore pressure, and with the soil retaining considerable reserves of strength and stiffness.

One explanation for the limiting level of excess pore pressure may be associated with upward drainage of the excess pore pressures. This is being investigated further.

CONCLUSIONS

1. A large data-set of the behavior of loose saturated sands under high initial effective confining stresses and subject to earthquake-like shaking has been collected during an extensive experimental program on the ERDC Centrifuge, Vicksburg MS.

2. This data has shown that, at moderate and high amplitudes of excitation, the maximum level of excess pore pressure development is limited at high initial effective confining stress and does not reach a level sufficient to cause 'initial liquefaction' (defined as 100% of the initial vertical effective stress).

3. These findings are currently being verified and will then be used to develop appropriate design guidance.

4. Rapid transmission of excess pore pressures from loose layers below has been found readily to lead to liquefaction of dense overlying layers.

5. The implication for the assessment of liquefaction hazard and requirements for remediation works under large earth dams is potentially very significant.

ACKNOWLEDGEMENTS

The ERDC Centrifuge Research Center and the Army Civil Works Earthquake Engineering Research Program of the U.S. Army Corps of Engineers sponsored this research. Richard Ledbetter, Director of the ERDC Centrifuge Research Center during the period of this research took a key role in the direction and accomplishment of this work. The members of the ERDC centrifuge team who helped conduct this work were Richard Burrows, Lee Miller, Dr Gary Butler, Rodgers Coffing, Wipawi Vanadit-Ellis, and Dr Mary Ellen Hynes. Drs William Marcuson and Michel O'Connor were Directors of the Geotechnical Laboratory. Permission to publish this paper by the Chief of Engineers is gratefully acknowledged.

REFERENCES

Arulanandan, A. and Scott, R.F. (1994) editors, Proc. Int. Conf. on Verification of Numerical Procedures for the Analysis of Soil Liquefaction Problems, at U.C. Davis; Volumes 1 & 2; Balkema.

Butler, G.D. (2000). A dynamic analysis of the stored energy angular momentum actuator used with the equivalent shear beam container, PhD thesis, Engineering Department, Cambridge University.

Byrne, P (2001). Private communication.

Steedman, R.S., Ledbetter, R.H., and Hynes, M.E. (2000). "The influence of high confining stress on the cyclic behavior of saturated sand", ASCE Geotechnical Special Publication No. 107, Soil Dynamics and Liquefaction 2000, Eds. Ronald Y.S. Pak and Jerry Yamamura,pp. 35-57.

Youd, L. and Idriss, I., Eds (1997) Workshop on Evaluation of Liquefaction Resistance of Soils, Proceedings, Salt Lake City, Technical Report NCEER-97-0022, sponsored by FHWA, NSF and WES, published by NCEER.

Zeghal, M., Elgamal, A.-W., Tang, H.T., and Steep, J.C., (1995). Lotung downhole array. II: Evaluation of Soil Nonlinear Properties, J. Geotech. Engrg., ASCE, 121(4), 363-378.